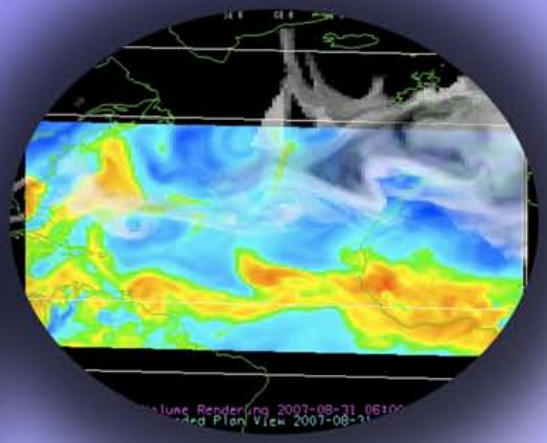

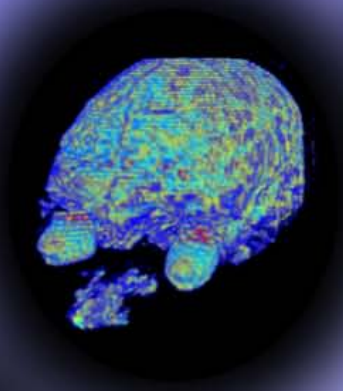

CS237
Final Project
Presentations

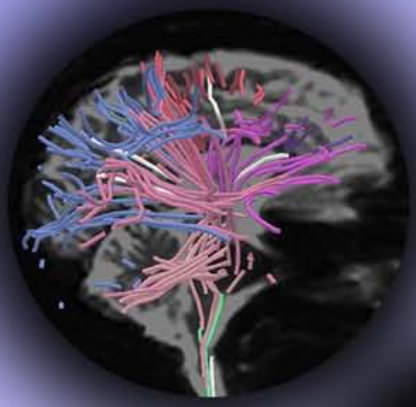

Thu, Dec 13, noon
Lubrano

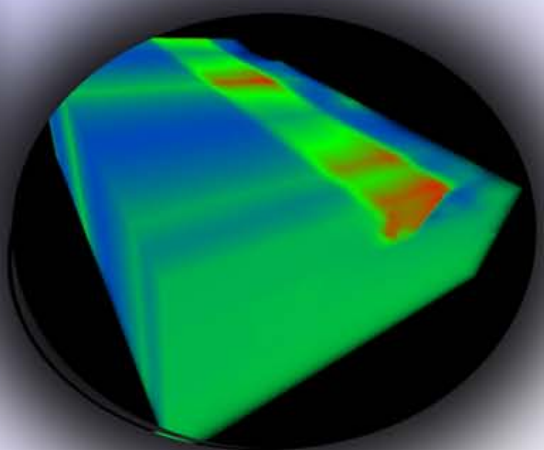

Significant Changes in Trapezoid and Trapezium Contact in the Scaphotapezio-Trapezoidal Joint as a Function of Kinematic Movement

+Wald, AJ[1]; Sevilla Lara, L[2]; Crisco, JJ[3]
[1]Dept. Of Biomedical Engineering, Brown University, Providence, RI [2]Dept. Of Computer Science, Brown University, Providence, RI [3]Dept. Of Orthopedics, Brown Medical School/Rhode Island Hospital, Providence, RI
andrew_wald@brown.edu

INTRODUCTION:

Past research has been able to show that the trapezoid and trapezium are closely bound to the scaphoid throughout the kinematic range of motions in the human wrist. It was once thought that the trapezoid and trapezium move along a single, fixed path that is relative to the scaphoid [1,2]. This, however, has been disproved by Sonenblum *et al.* [3]. The consequences of this theory give rise to the idea that the trapezoid, trapezium, and scaphoid, the scaphotrapezio-trapezoidal (STT) joint, undergo more complicated motions than previously thought. It then becomes necessary to examine, in greater detail, the true movements of the trapezoid and the trapezium relative to the scaphoid during a full range of kinematic poses.

Through the use of a novel visualization technique that incorporates both a broad view of the carpal bones as well as specific bone detail, we were able to investigate cartilage contact areas that were approximated by fixed distance contours through a range of carpal bone motions. While investigating contact areas between bones in the carpal STT joint, we have found evidence of significant change in both the area and position as kinematic motion fluctuates over a broad range of poses.

METHODS:

All data was taken from a digital data base of wrist bone anatomy and carpal kinematics, and the data that was used in this case consisted of both male and female non-pathological subjects. Using a combined motion protocol, the data was acquired by computed tomography (CT) with the subjects undergoing motions to target levels of flexion, extension, radial deviation, ulnar deviation, and all of the possible combinations of those movements. The true values of flexion, extension, ulnar deviation, and radial deviation were calculated by utilizing a an inertially-defined coordinate system with the angles of movement clinically defined [5]. From this point, the carpal bones were segmented and their surfaces were reconstructed, while the kinematic transforms were all produced by the procedure described in Moore *et al.* [4]. Distance field maps were then created for each bone as a function of kinematic pose. The calculated distance map between the bones allowed for the creation of contours at set levels of 1 mm to 5 mm, at intervals of 1 mm, for each position. By examining the path of the contours on the bones and their areas as a function of motion based on the combined motion kinematic positions we, were able to observe a few trends that help characterize carpal bone motion in the STT complex.

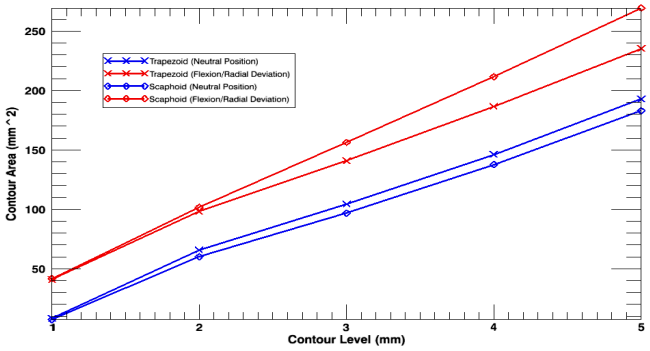

Figure 1: Changes in contour area as a function in the clinically neutral position compared to large values of flexion and radial deviation.

RESULTS:

By observation, for both subjects, the change in contour area as a function of kinematic position is significant. Figure 1 shows a typical subject, and the values of the contour areas, for the trapezoid and scaphoid, as a function of a change in kinematic position from the clinically neutral position to large values of flexion and radial deviation. For this subject, the amount of flexion was 14.42º while the amount of radial deviation was 17.27º.

The contoured contact areas also tended to undergo a significant shift in position and change in area magnitude as a function of carpal kinematic position. Figure 2 displays a typical example of a scaphoid and its contact areas with the trapezoid over a few poses in the kinematic range of motion.

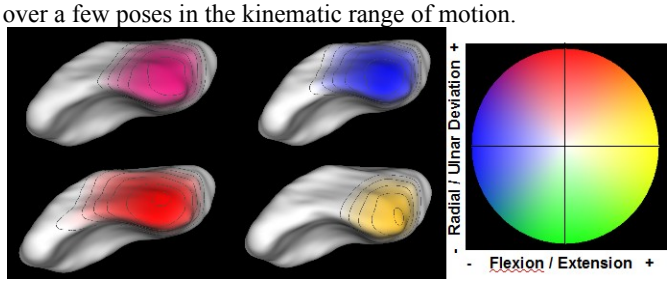

Figure 2: A typical shift in contour contact area positions on a scaphoid, relative to a trapezoid, for a sample of kinematic motion target positions.

DISCUSSION:

The reiteration that the STT joint undergoes complex movements, rather than tracking on a single line is important in understanding the more complicated carpal bone movements in the wrist. Using a novel visualization that afforded both a global view of wrist kinematics, and vital inter-bone distance detail on the single bone level, provided a way to further analyze carpal motion in the STT joint.

By examining the areas of fixed-level contours, we have been able to show that inter-bone distances not only change in magnitude, but also, they shift in their positions as a function of overall wrist position. This idea gives rise to the possibility that utilizing distance fields at fixed levels between bones could serve as a fairly solid approximation for articular cartilage contact.

Additionally, more subjects must be analyzed to ensure that the trends mentioned continue. The analysis methods that should occur would involve statistical calculations to determine whether or not the phenomena observed is truly related to global wrist motion. Also, it is possible that different subsets of populations will have different changes with regards to their contact areas, and the positions of their contact areas based on kinematic position of the wrist.

REFERENCES:

(1)Moritomo, et al. J Hand Surg 25:911-920 2000a (2)Kauer JM. Clin Ortho and Rel Res 202:16-26 1986 (3)Sonenblum, et al. J Biomech 37:645-652 2004 (4)Moore DC, et al. J Biomech 40:2537-2542 2007 (5)Coburn JC, et al. J Biomech 40(1):203-209 2007

Interactive Display and Analysis of Local and Global Changes In Carpal Bones Throughout a Full Range of Kinematic Motion in the Human Wrist

Sevilla Lara, L[1]; Wald, A[2]; Crisco, JJ[3].

Dept. of Biomedical Engineering, Brown University, Providence, RI
Dept. of Computer Science, Brown University, Providence, RI
Dept. of orthopedics, Brown Medical School/Rhode Island Hospital, Providence, RI

Researching the independent behavior of each of the carpal bones as a function of the overall wrist kinematics represents a scenario where the depiction of global and local data should be studied in depth. Both general and detailed information need to be displayed at the same time to permit complementary insight. This will allow robust investigation of the movement of the bones, to gain knowledge that can be applied to many pathologies.

We have developed a tool that successfully enables this task, providing information about bone positions, ligaments, and areas with the same inter-bone distances.

I. INTRODUCTION. Motivation

Previous studies have proven that bones move independently while the complete wrist performs a larger scale movement. This leads to a change in the distance between the bones as a function of the overall position of the wrist. This distance is an important aspect to study in order to gain insight about the wrist kinematics, which will help understanding numerous pathological conditions.

At the same time, visualizing the ligaments, their insertions and origins, and their elongation along different poses of the wrist allows a better comprehension of the carpal bone motion due to the mechanical constraints that they place on the bones.

This behavior provides a perfect scenario to identify one of the top scientific visualization problems described by C. Johnson [1]. This problem comprises the simultaneous depiction of *global and local data*, in order to provide information about the system as a whole (in this specific domain, the wrist), while showing details about the different parts that compound the group (in this case, each of the carpal bones).

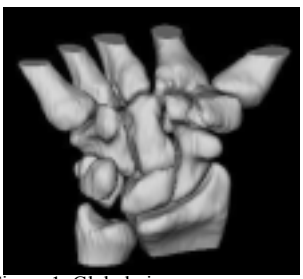

Figure 1. Global view

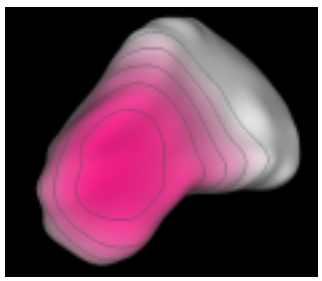

Figure 2. Local view including distance isocontour

II. SPECIFIC AIMS.

Hence, this project's main goal is to tackle the visualization problem of displaying global and local data, applied to the study of the movement of bones in wrist kinematics.

Within this scope there are some more specific objectives: visualizing at the same time the position of the wrist and the position of the bones that compound it; showing the ligaments and their elongation; and displaying the inter-bone distance for every given position.

Once these tasks have been accomplished, the last aim of the project is to explore the behavior of the particular bones. More specifically, trapezium, trapezoid and scaphoid represent the more interesting part of the study.

III. METHODS

To accomplish our purposes, we have developed a software tool based on an already existing one [2] that provided the ability to show the complete wrist. We updated it by integrating the partial view of each bone for different positions, using *C#* and the *.NET platform*. This new feature allows the user to explore the kinematics of every bone in depth, without losing the perspective of the global situation. Partial views can be removed to avoid overload of information.

Inter-bone distances are displayed using *isocontours*. This technique encloses the areas of the bone whose distance to the next adjacent bone is within the same range, typically 1 mm. as developed by [3]. Also, colors are used to give a perceptual idea of the proximity, increasing the intensity of the color in between contour lines as distance decreases.

These inter-bone distances are calculated using a method that calculates *distances maps* around every bone to accelerate the process of computing the final absolute distances.

Finally, ligaments are displayed using streamtubes. There is also the ability to remove this data from the screen, to prevent overlapping and overwhelming.

VI. RESULTS. Conclusion

The final platform created enables a simultaneous view of the data at a global scale as it can be seen in figure 1, while showing local position of the bones as it can be seen in figure 2, where also inter-bone distances are represented. Finally, ligaments are shown in figure 3.

The product developed in this project constitutes a valid solution for the scientific visualization problem stated. Furthermore, it is a consistent framework for future research on carpal kinematics, specially due to its design based on the necessities of this particular domain study.

V. REFERENCES

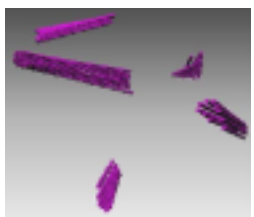

Figure 3. Streamtubes for ligaments representation

[1]C.Johnson.Top Scientific Visualization problems. *IEEE Computer Graphics and applications, 2004*

[2] 2. DC Moore, JJ Crisco, TG Trafton and EL Leventhal. A digital database of wrist bone anatomy and carpal kinematics. Journal of Biomechanics, 40(11):2537-2542, 2007

[3] "Interactive Visualization of 3D Carpal Kinematics and Bony Anatomy" JJ. Crisco, C. Demiralp, D. H. Laidlaw,Scientific Exhibition, ASSH 56th Annual Meeting, Baltimore, MD, October 2001

Hierarchical Selection Methods for DTI Fiber Bundles

Ahmad Wilson and Matt Loper
Brown University, Providence, RI

Stephen Correia
Butler Hospital, Providence, RI

Currently, there are several methods for region of interest selection among DTI Fiber bundles [1] [2] [3]. These existing selection methods, which generally involve utilizing boxes or multiple polyhedral convex objects to target a region of interest, however, do not always adequately encapsulate the irregular shapes and curvature exhibited by these bundles. Furthermore, these selection techniques can prove to be quite difficult in cases where bundles are obscured by other bundles, as is often observed. Therefore, we present an automatic, interactive method based on a simple form of hierarchical selection. This method not only overcomes the deficiencies of these existing methods but also provides an easier, more user-friendly interface for examining fiber tracts.

I. METHODS

Our selection methods are built on top of the BrainApp platform developed by Zhang et al. Once the selection process is initiated, the entire brain, more precisely, the streamtube representations of its fiber tracts, will be set to a single default color/bundle. Upon cursor-based selection, further cluster refinement will occur on the selected bundle. That is, the selected bundle will be subdivided into two colors/bundles based on our clustering algorithm [1] - (see figure 1). Furthermore, we provide the user with the supplemental capability of deactivating or making less visible regions of disinterest by simply, with a click of the middle mouse button, hiding these regions from the user's view – (see figure 2).

II. RESULTS

The primary goal of this project is to help segment fiber bundles that possess complex trajectories, and, as a result, are generally difficult to select utilizing existing region of interest selection methods. Specifically, there are two pathways of interest for this project: the fronto-parietal segment of the superior longitudinal fasciculus, associated with working memory abilities, and, the uncinate fasciculus, associated with working memory as well as emotional memory. Behind an expert-driven comparison with

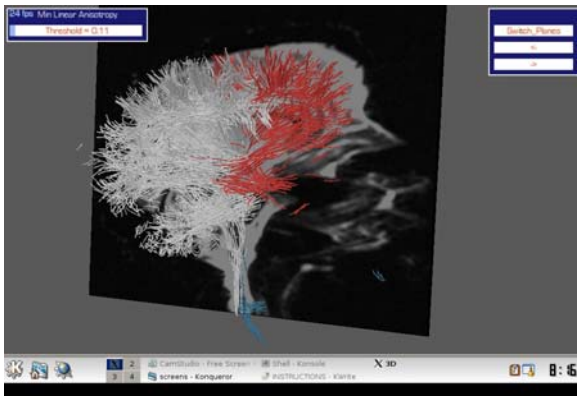

Figure 1: Based on our hierarchical selection feature, the fiber tracts have been segmented into three individual bundles.

Figure 2: The red region visible in figure 1 has been hidden by the user in order to better focus on regions of interest

BrainApp's current box selection method, we evaluated how well this tool could be used, both quantitatively and qualitatively, to assess the structural integrity of these fibers in patients with an inherited form of subcortical ischemic vascular dementia, which is characterized by working memory impairments. Our results were as follows:

Uncinate Fasciculus	**Our Method**	**Box Method**
Time to find	**3:27**	**9:45**
Ease of use	**2**	**4**
Confidence in tract selection	**2**	**2**

Table 1: Time is in minutes and seconds. Ratings are on a scale from 1-5 with 1 being the best and 5 being the worst. Also note: due to a bug within our application, we were unable to complete the comparison tests on the superior longitudinal fasciculus.

III. CONCLUSION

In conclusion, overall, our results indicated that users, who had considerable experience utilizing the box selection method, were able to locate specific regions of interest at a significantly faster rate using our method than when using the box method. Furthermore, while obtaining an identical "confidence in tract selection" rating as the box method, our application was deemed to be generally easier to use and more straightforward. One user described the experience as both "colorful" and "enjoyable". These initial results demonstrate the promise our method holds in enhancing future DTI- related research.

IV. REFERENCES

[1] Song Zhang and David Laidlaw "Hierarchical Clustering of Streamtubes", [2] Anthony Sherbondy "Exploring Connectivity of the Brain's White Matter with Dynamic Queries", [3] Jorik Blaas "Fast and Reproducible Fiber Bundle Selection in DTI Visualization"

Hierarchical Selection Methods for DTI Fiber Bundles

Matt Loper, Ahmad Wilson
Department of Computer Science
Brown University
{matt}{awilson}@cs.brown.edu

Stephen Correia
Department of Psychiatry and Human Behavior
Brown University
{scorreia}@butler.org

I. Introduction

We propose a new method for the hierarchical selection of bundles in the brain. Researchers wish to find these anatomical bundles in MRI datasets in order to measure their strength and connectivity. Current methods for selection generally involve intersecting halfspaces and simple geometric shapes [1], [2], which do not conform to the natural layout of axonal tracts. We cluster the tracts hierarchically, and allow a user to recursively find a bundle of interest. In comparison to a box-based method, we found that our approach improves time to selection and ease of use.

II. Methods

In our preprocessing step, streamtube generation and clustering are accomplished in the manner of Zhang et al [3]. Streamtubes are generated from a 256 x 256 x 50 data set. After streamtube generation, each tube is assigned to its own singleton cluster. Clusters are then joined, one by one, according to a distance metric, until a complete binary tree of streamtubes is constructed. We adapted the first method of [3] for our distance metric, though any distance metric could be used. These N x N distances are also precomputed and stored.

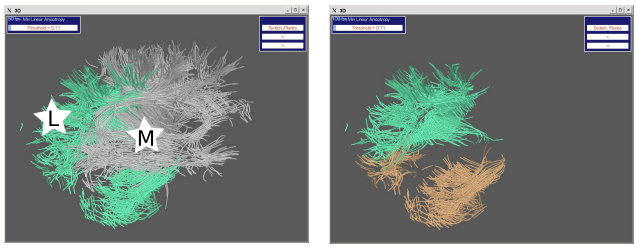

Fig. 1. A left click subdivides the green cluster into green and orange. A middle click removes the gray cluster. Mouse clicks are denoted with stars.

During runtime, a user is allowed to interact with (zoom, translate, and rotate) the streamtubes. The brain is initially segmented into two differently-colored bundles. A mouse click on any cluster will subdivide it into two differently colored subclusters, according to the precomputed tree. Individual bundles may also be hidden or shown by using a middle mouse click.

III. Results

Our approach was evaluated by a neuroscience concentrator at Brown University. This subject is experienced with box-based selection. Three criteria were considered: user selection time, ease of use, and confidence in selection. User selection time was measured in minutes. Ease of use and confidence were measured on a Likert scale. Ease of use ranged from 1 (intuitive, simple to interact with) to 5 (cumbersome, unintuitive, hard to correct mistakes). Confidence of selection ranged from 1 (highly confident, no more or less fibers than necessary) to 5 (false positives or false negatives are difficult to avoid). These criteria were applied to our approach and (for purposes of comparison) to a box-based selection mechanism.

Two bundles were selected during evaluation: the superior longitidudinal fasciculus (SLF), and the uncinate fasciculus (UF). These bundles were selected because collaborating researchers are interested in them and because their curvy trajectory makes them challenging to segment. After a few practice runs on a training dataset with both methods, the criteria were evaluated with a second dataset.

TABLE I
Task times and qualitative criteria are compared with those of a box-based method.

	Our method	Box-based method
Time to selection	3:27	9:45
Ease of use	2	4
Confidence	2	2

Table I shows our results on selection of the UF. Results on the SLF are omitted, as a ray-intersection bug required us to abort that task. Anecdotally, the rater found our method easier and faster to use on the training dataset as well.

In our experimental setting, our system was found to be superior in the areas of ease of use and time to selection, while achieving confidence equivalent to that of a box-based approach. Informal comments suggested that our method was experientially more pleasant than the box-based method.

IV. Conclusions

We believe that our approach will make bundle selection faster and easier, thereby accelerating DTI-related research on the brain. The pathways of interest (UF and SLF) are currently being studied by Dr. Correia in patients with a disorder known as CADASIL (cerebral autosomal dominant arteriopathy with subcortical infarctions and leukoencephalopathy); the use of our approach may have immediate benefits on the pace of that study.

V. References

[1] Jorik Blaas, Charl P. Botha, Bart Peters, Frans Vos, and Frits H. Post. Fast and reproducible fiber bundle selection in DTI visualization. In *IEEE Visualization*, page 8. IEEE Computer Society, 2005.

[2] Anthony Sherbondy, David Akers, Rachel Mackenzie, Robert Dougherty, and Brian Wandell. Exploring connectivity of the brain's white matter with dynamic queries. *IEEE Transactions on Visualization and Computer Graphics*, 11(4):419–430, 2005.

[3] Song Zhang and David H. Laidlaw. Hierarchical clustering of streamtubes. Technical Report CS-02-18, Brown University Computer Science Department, August 2002.

Exploratory Visual Analysis of Earthquake Simulation Data

Brandon Nardone (PI) Scott Daniel (Co-PI) Terry Tullis (Collaborator)
Brown University, Providence RI - December 14, 2007

Introduction

In an effort to better understand and ultimately be in a position to accurately predict earthquakes, geoscientists attempt to define mathematical models for the behavior of seismic activity. Simulations are run against these models so as to determine the accurateness of these models.

One such simulation is run by Prof. Terry Tullis against the Parkfield section of the San Andreas fault. The results of these simulation runs are time-varying scalar data on a non-uniform grid.

We present methods to visualize these results as well as a free, light-weight implementation.

Methods

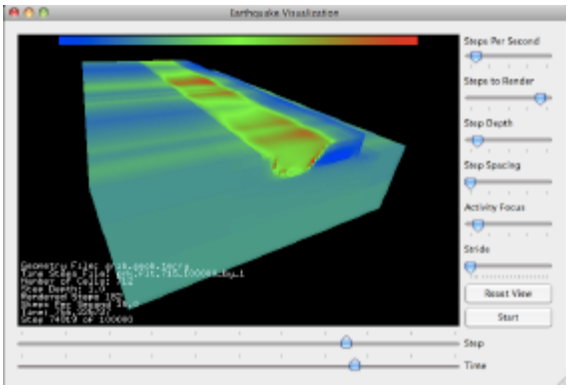

Figure 1: Screen capture of application in use. Color scale on top represents relative values of slip rates from decreasing to increasing.

We apply well-studied visualization methods including color and transparency mapping and volume rendering to the visualization of earthquake fault slip rates.

Real-time configurable color mapping is implemented allowing for attention to be drawn to relatively or absolutely high slip rates between the plates. Transparency of each cell is a function of its slip rate as well as the current time steps proximity to the time step of interest. This helps to draw attention to high slip rates as well as to the time step currently in focus.

Volume rendering, in conjunction with the above methods, allows for investigation into temporal as well as spatial patterns in the data set. Nearly all parameters going into the generation of the rendering are exposed to the user and changes are reflected in realtime.

Furthermore, the user is allowed to select a point on the current time step of interest. Through the use of a sensitivity slider, the application then removes all non-associated activity from view by searching from the selected point in time and space. Those cells whose difference in slip rate from their selected peers is greater than the threshold are culled.

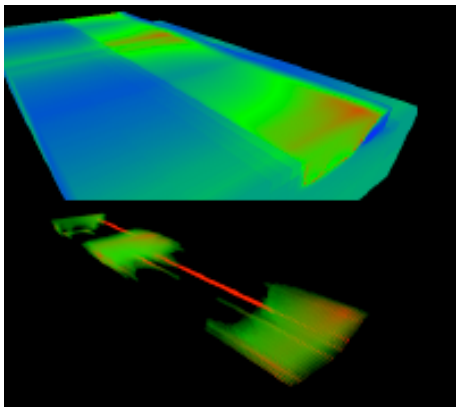

Figure 2: Activity of interest selection.
Top: Volume rendering of data set.
Bottom: Rendering of relative slip rates related to selected point.

Results

The implementation of the proposed methods was a complete success from a software perspective.

We are presently working with our collaborator to investigate the utility of our visualization application. The initial response has very positive. Anecdotal feedback is also being collected from others in the field.

References

[1] *Visualizing Very Large-Scale Earthquake Simulations*, Ma, Kwan-Liu et al., 2003,
Proceedings of the ACM/IEEE SC2003 Conference
[2] *Immersive Volume Visualization of Seismic Simulations: A Case Study of Techniques Invented and Lessons Learned*, Chopra et al., 2002, 13th IEEE Visualization 2002
[3] *Use of fast multipoles for earthquake modeling,* Tullis, T. E. et al, 2000

Volume Rendering of Time-Varying Earthquake Simulation Data

Scott Daniel, Brandon Nardone
Department of Computer Science
Brown University

Terry Tullis
Department of Geological Sciences
Brown University

Introduction

We have proposed a new tool for visualizing the output of earthquake simulations in order to help geologists better understand earthquake phenomena. In particular, we developed our tool in collaboration with Dr. Tullis of the Geology department at Brown University to allow him to observe spatial and temporal patterns of slip rates in earthquake faults. Ultimately, the purpose of our tool is to help Tullis and others in the geological community visually analyze seismic activity.

Currently, Dr. Tullis' data exists as non-uniformly sized cells in grids of slip rate data spaced non-uniformly in time. He uses a general purpose data visualization program to visualize his data. Unfortunately, this tool only renders Tullis' data one time step at a time which makes it insufficient to be of use to him. Our tool allows Tullis to interactively explore the temporal relationships between multiple time steps of seismic activity. In addition, our tool helps Tullis identify regions of interest through color and transparency mapping.

Methods

To assist Dr. Tullis in visualizing the temporal relationships within his slip rate data we display a volume rendering of a sequence of time steps (*Figure 1*). Our method spaces the time steps evenly along an axis of increasing time. The slip rate cells within a time step are color and transparency mapped based on the magnitude of their slip rate and are then rendered out as voxels.

In addition, we have added time step animation to help the user visually analyze the change in slip rates from one time step to the next. The user has various options to select the time intervals of interest, number of slices to render, and playback rate of the animation.

To enable the user to distinguish between the different slip rates in each time step we used a color mapped approach. The slip rates of each cell within a time step can be color mapped in two different fashions. The first method is to color map each cell based on its relative slip rate magnitude to the to maximum slip rate of the entire data set. The second method assigns the cell 's color based on its relative slip rate magnitude to the maximum slip rate of its corresponding time step. The two color mapping methods allow for the viewer to see the global relationships of all the slip rates and the local relationships of slip rates in the same time step as well.

We also enable the user to highlight particular regions of interest by removing uninteresting ones through an optional transparency mapping. In this fashion slip rates of smaller magnitude are rendering more transparent than larger slip rates. Additionally, time steps that are further away chronologically from the current time step are rendered at lower opacity than time steps closer to the current one. This additional functionality makes slip rates in the current time step more salient than those in the future.

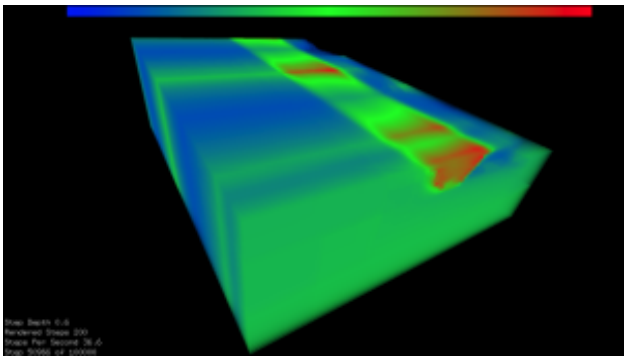

Figure 1: A volume rendering of multiple time steps of slip rate data

Results

Our earthquake visualization tool enables users to interactively visualize multiple time steps of slip rate data sequentially. Using our method various time steps may be analyzed from different vantage points and magnified to examine detail in real time.

Thus far we have received positive and enthusiastic feedback from our collaborator about our work. He believes that in its current state our tool is a better alternative to his current data visualization program. From a tool smith's perspective we have successfully achieved our goal as computer scientists by meeting the needs of our collaborator.

Conclusion

Although we have developed a tool for visualizing earthquake simulation data in an effective manner there are still improvements that can be made. We have received suggestions from our collaborator about features that would make our tool more useful from a scientist's point of view. This idea suggests that there is more work to be done in this area.

References

[1] Tullis, T.E. et al, Use of fast multipoles for earthquake modeling, 2000

[2] Hansen, Charles D. and Chris R. Johnson. Visualization Handbook. Oxford: Elsevier, 2005.

[3] Frederick P. Brooks, Jr., The computer scientist as toolsmith II, Communications of the ACM, March 1996

Visualization of Uncertainty in Atmospheric Advection and Current Interaction during Atlantic Hurricane Formation

E.J. Kalafarski, R.A. Boller, and D.H. Laidlaw, Computer Science Department, Brown University
S.A. Braun, Mesoscale Atmospheric Processes Branch, NASA/Goddard Space Flight Center

Introduction

Global atmospheric circulation data now available from NASA's Goddard Space Flight Center[1] provides a novel opportunity to identify factors that influence and contribute to hurricane development in the Atlantic Ocean. Much work has been done on these individually, especially in the hurricane "breeding ground" off the western coast of Africa[2], but their effects and the influence of other remote air sources are still unclear. Specifically, we seek to understand the interactions of dust off the Saharan Air Layer with other potential sources of warm, dry air that may contribute to the process of cyclogenesis.

We apply the visualization of uncertainty to back-trajectory analysis, a versatile method of extrapolating the sources of a storm system by tracing back in time along the wind field. In doing so, we address the lack of confidence in meteorological visualization, as well as the uncertainty and clutter implicit to back trajectory generation.

Method

The use of back trajectory analysis is not new to the field[3], and we accomplish it with the Runge-Kutta class of algorithms and the pathline, a continuous line tracing the route of a single particle through a dynamic vector field. A cluster of pathlines can demonstrate the interactions of air parcels during storm formation. While back trajectory analysis is used often to identify sources of storms, it is an approximation and thus carries an inherent margin of uncertainty. We address this explicitly by presenting a versatile interface which allows a researcher to generate a set of back trajectories which indicate confidence levels in themselves and express properties of the parcel.

A meteorologist studying hurricane formation is presented with a map allowing manual selection of a region of interest, from which a set of pathlines are seeded. The pathlines are generated from each seed point, advecting backwards through time over a changing wind vector field, the Global Circulation Model (GCM). Uncertainty is presented in a manner that allows the meteorologist to evaluate likely sources using both confidence in a trajectory, indicated by pathline thickness, and properties such as humidity, indicated by color along the pathline. Opacity, in turn, provides the researcher a method of focusing on pathlines in more interesting areas of high turbulence. These tools provide the researcher with a more complete picture in which more credence can be placed.

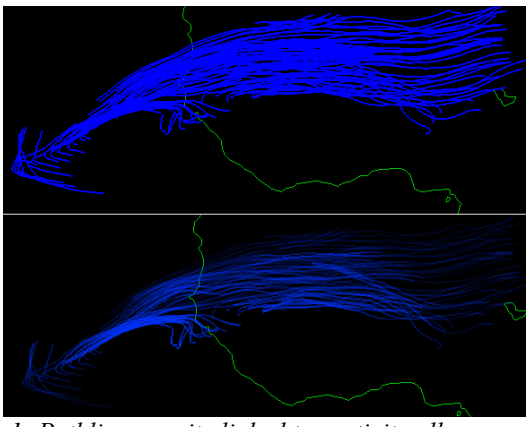

Figure 1: Pathline opacity linked to vorticity allows a user to focus visually on more useful regions of high turbulence.

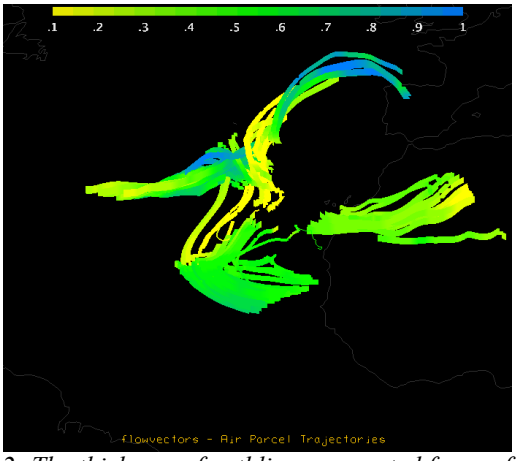

Figure 2: The thickness of pathlines generated from a forming hurricane indicates their confidence levels, while color conveys the humidity of the combining parcels.

Conclusion

Specific to our goals, the features of air parcels before they combine are of particular import, and researchers can now identify air sources of a storm system of interest based on their properties and prior trajectories. These tools are particularly well-suited to the study of currents off the Saharan Air Layer, parcels crucial to the process of hurricane formation which are well-understood in their compositions but not in their interactions.

We have provided the meteorologist with a method for manually selecting a region of interest and extrapolating its source or sources, indicating simultaneously the properties of the advected parcels and the confidence in the end result. The researcher also has a new method with which to "peel away" layers of trajectories to focus on air parcels of note and reduce clutter. These tools present methods which should be helpful in the ongoing process of predicting the path and intensity of hurricanes through the understanding of cyclogenesis.

References

[1] Collins, N. et al. 2005. *Int. J. High Perform. Comput. Appl.* 19, 341–350.
[2] Dunion, J.P., et al. 2004. *Bull. Amer. Meteor. Soc*, 85, 353–365.
[3] Chen, L.W.A. etal. 2002. *Atmospheric Environment*, 36, 4541-4554.
[4] Hibbard, B. 2000. SIGGRAPH Comput. Graph. 34, 1,40-40.
[5] Park, S.W. et al. 2005. EUROGRAPHICS – IEEE VGTC Symp. on Vis.

Explicitly and Implicitly Representing the Confidence of Air Parcel Trajectories in Meteorological Research

R.A Boller, E.J. Kalafarski, and D.H Laidlaw, Dept. of Computer Science, Brown University
S.A. Braun, Mesoscale Atmospheric Processes Branch, NASA/Goddard Space Flight Center

1 Introduction

In this work, we use a Global Circulation Model[1] to identify factors that contribute to hurricane development in the Atlantic Ocean. Two such factors are dust and hot, dry air from the Saharan Desert. Their effects are heavily studied[2][3], but it is unclear whether alternate sources of warm, dry air also contribute.

Back trajectory analysis[4] is a common meteorological technique used to determine the source location of an air parcel at some previous time step and is applied to this problem. While these analyses provide a good approximation of the air parcels' paths, the oft-overlooked problem of *identifying and representing sources of potential uncertainty*[5] is addressed. The pathlines are a derived quantity, but the accuracy of their derivations[6] are rarely represented. We develop two methods to identify and show confidence in these pathlines.

2 Methods

By performing back trajectory analyses, we identify alternate sources of hot, dry air, along with observing interactions when these paths wrap into storm circulations. To visualize this path over time, a set of pathlines are seeded at the air parcel's final location, then are advected backward through time using a 3-D grid of wind vectors (Figure 2). To then provide the meteorologist with a measure of confidence in these results, the amount of uncertainty from interpolation is shown.

Interpolation uncertainty is introduced when fitting paths to a relatively coarse uniform grid and through areas of rapid change. This is explicitly represented on a per-pathline basis through their widths: thinner pathlines represent less confidence than fatter ones, inherently highlighting the more accurate pathlines. Note that further uncertainty is introduced during numerical integration of the parcel paths through the wind vector field, but is not addressed in this study.

We then apply occlusion reduction techniques[7] to dense pathline bundles to aid in highlighting the implicit confidence level shown by the divergence of the pathlines themselves. By reducing homogenous, redundant information, we show underlying features that would have otherwise been obscured.

In the end, the aim of this explicit and implicit uncertainty representation is to provide a clearer understanding of these simulated paths and the processes they represent, giving the scientist more confidence in the generated results.

3 Results

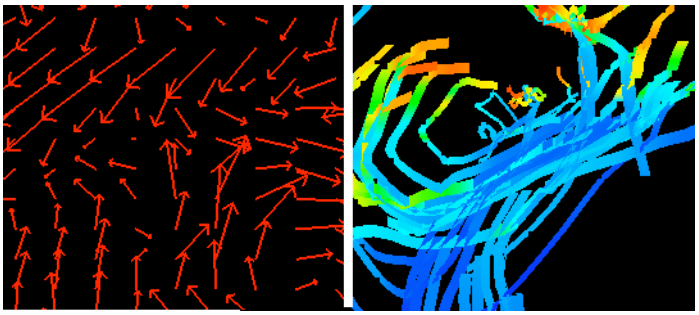

Figure 1: One time step from vector field (left) used to generate pathlines (right). Note wind shear in center of field and its effect on trajectory confidence.

In Figure 1, a set of pathlines and one of its underlying vector fields are shown. The width of each pathline is adjusted according to the level of confidence in its interpolation, revealing bundles of pathlines in areas of high wind shear that are untrustworthy. The pathlines are colored according to their relative humidity, showing a "snapshot" of its value in time, helping to find sources of dry air.

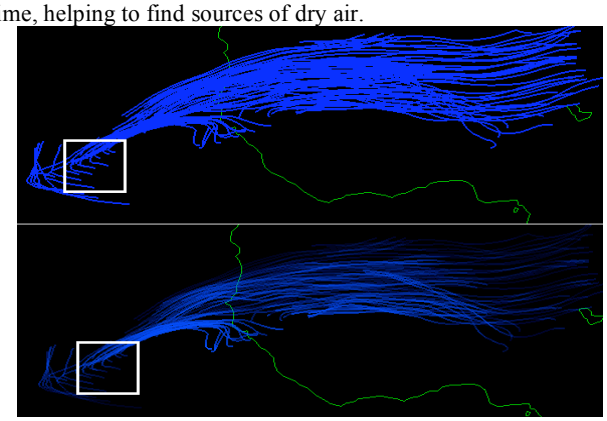

Figure 2: Fully opaque pathlines (top) vs. those with opacity mapped to vorticity, revealing turbulent regions more clearly. White box shows seeding area.

Figure 2 illustrates the advantage of mapping pathline opacity to vorticity: turbulent regions are shown more clearly. This is performed on a per-vertex basis, allowing the turbulent regions of a given pathline to be highlighted while the steady parts are de-emphasized, having the overall effect of reducing occlusion.

4 Conclusions

Through this work, we show that the representation of trajectory uncertainty provides users with an extra layer of confidence in their results. It quickly highlights geographic regions where interpolation uncertainty produces pathlines that are not realistic. It also reveals underlying features by removing redundant information, taking advantage of the implicit confidence shown naturally by the amount of pathline divergence.

Furthermore, the adoption rate of 3-D visualization tools by meteorologists has generally been slow due to skepticism of new methods [8] and lack of quantifiability [9]. From our work, we aim to take a step toward alleviating these concerns and provide tools that take advantage of the capabilities of new technology and techniques.

5 References

[1] Collins, N. et al. 2005. *Int. J. High Perform. Comput. Appl.* 19, 341-350.
[2] Dunion, J.P., et al. 2004. *Bull. Amer. Meteor. Soc.*, 85, 353–365.
[3] Karyampudi, V.M. et al. 2002. *Mon. Wea. Rev.*, 130, 3100–3128
[4] Chen, L.W.A. et al. 2002.*Atmospheric Environment* 36, 4541–4554.
[5] Johnson, C. R. et al. 2003. *IEEE Comput. Graph. Appl.* 23, 5, 6-10.
[6] Lopes, A. et al. 1998. Mathematical Visualization: Algorithms, Applications and Numerics, *Springer Verlag*, pp. 329-341.
[7] Park, S.W. et al. 2005. *EUROGRAPHICS - IEEE VGTC Symposium on Visualization*
[8] Hibbard, B. 2000. *SIGGRAPH Comput. Graph.* 34, 1, 40-40
[9] Tufte, E.R. 1997. *Graphics Press*, pp. 20-23.

The Relationship Between Cell Topography and Neural Growth: A Computational Approach

Trevor M. O'Brien
Brown University
Department of Computer Science
trevor@cs.brown.edu

Jan M. Bruder
Brown University
Department of Biomedicine
jan_bruder@brown.edu

David H.Laidlaw
Brown University
Department of Computer Science
dhl@cs.brown.edu

I. Introduction

To induce in-vivo nerve regeneration, researchers are currently exploring and measuring the effects of various factors that contribute to neural growth. In this work, we introduce an exploratory visualization tool for analyzing the relationship between neural growth and one such factor: cellular topography. To examine this relationship, confocal microscopy image stacks containing two cell types, Schwann cells and neurons, are reconstructed in 3D and statistically analyzed. Understanding the relationship between these cell types with respect to proximity, orientation, and relative size is critical to current regenerative neural growth studies.

In the confocal microscopy image stacks analyzed in this work, it was statistically confirmed that neurons chose to align themselves quite strongly with underlying Schwann cells. Further, in expert evaluation, the visual techniques employed in this study were found to facilitate data exploration and potentially lead to new hypotheses regarding neural growth.

II. Methods

A. Isosurface Extraction

The confocal microscopy image stacks are first reconstructed as a three-dimensional volume. Connected point clouds within this volume are determined, and isosurfaces are extracted for each of the connected components. These segmented isosurfaces represent cell boundaries, and serve as the basis for our analysis.

B. Quantitative Analysis

Principle component analysis (PCA) is performed on each segmented cell. The orientation of a collective group of cells is determined in a weighted mean sense, with weights being determined by the size of the cell. To compare alignments of two groups of cells, an alignment score is calculated based on the absolute value of the dot products of the two groups' collective directional vectors.

To assess health of cells, other statistics are computed and output for further analysis. These measures include total cellular surface area, inter- and intra-cell-type distances, and an approximation on cell volume.

C. Visualization

In one visual mode, cell surfaces are rendered along with thin cylinders representing their primary principle component. Cells for which no dominant primary component exists – cells that are pancake-shaped or spherical – are accompanied by a semi-transparent sphere rather than an aligned cylinder.

A second visual mode allows for the rendering of the primary principle components only, without cell surfaces. This visualization technique is analogous to a 3D vector field and may lend itself nicely to future studies of neural growth over time.

Lastly, a third mode exists to highlight variation in cellular orientation. For a given group of cells, each connected component is colored according to its directional agreement with the cells' collective alignment. The colormap ranges from blue to red, with blue representing cells that are closely aligned, and red representing regions that are orthogonal to the collective alignment. Adding to the exploratory nature of this visualization tool, the user has interactive control of the sensitivity for this colormap.

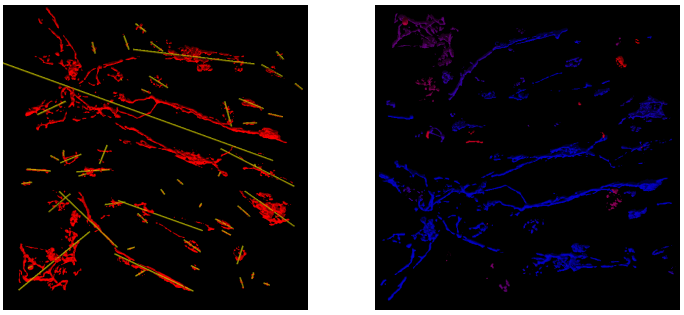

Fig. 1. (Left) Neuron isosurfaces with their primary principle components rendered as yellow cylinders. (Right) Segmented neurons colormapped according to their directional agreement with the cells' collective alignment.

III. Results

Statistical results from the 3D analysis performed in this application were compared directly to results obtained using a state-of-the-art image analysis techniques similar to those seen in [1]. It was evident from this comparison that 2D analysis of a representative slice from a confocal microscopy image stack is not sufficient for extracting meaningful quantitative results. The results of a comparison from one such data set can be seen in the table below.

	Schwann Dir.	Neuron Dir.	Agreement
3D:	(0.78, 0.48, 0.01)	(0.85, 0.12, 0.03)	0.92
2D:	(0.69, 0.45)	(0.68, 0.22)	0.56

IV. Evaluation

This tool was evaluated by a group of biomedicine doctoral students who are familiar with confocal microscopy image analysis. Overall, they were extremely impressed with the visualization application, including both its quantitative and exploratory aspects.

They made the point clear that three dimensional analysis is critical to furthering their research, and adopting this tool will allow them to statistically support or negate many of their hypotheses.

They also found the display of variation in orientation to be clear and intuitive. They believed this feature had the potential to lead to further hypotheses about neural growth.

V. References

[1] Jan M. Bruder, Andrea P. Lee, and Diane Hoffman-Kim. Biomimetic materials replicating schwann cell topography enhance neuronal adhesion and neurite alignment in vitro. *Journal of Biomaterials Science, Polymer Edition*, 18(8):967–982, August 2007.

Connective Coherence: A Distributed Measure for White Matter Integrity

Jadrian Miles*, Stephen Correia†, and David H. Laidlaw*
* *Department of Computer Science, Brown University, Providence, RI, USA*
† *Department of Psychiatry and Human Behavior, Butler Hospital, Providence, RI, USA*

We define a property called *connective coherence* that measures the effect of internal structure upon diffusion between two volumes of interest within an arbitrary diffusive medium. We hypothesize that this may be used as a meaningful measure of brain white matter integrity in the study and diagnosis of psychiatric pathologies such as post-traumatic stress disorder and schizophrenia. In order to validate this hypothesis, we designed a software application to visualize the brain and select cortical regions of interest for analysis. This progress prepares us to perform comparative clinical studies between brain scans of diseased and healthy patients. A significant difference in connective coherence between these groups would be a step toward confirming our hypothesis.

I. Background

The white matter (WM) is fibrous tissue in the interior of the brain that conveys signals between regions of the cortex, the outer layer of brain tissue. Integrity is the qualitative notion of the strength of a given WM connection, degradation of which is hypothesized to play a role in many psychiatric pathologies, including post-traumatic stress disorder, schizophrenia, kleptomania, and late-life cognitive degeneration [7], [3], [4], [2].

Various quantitative characteristics of brain tissue derived from non-invasive diffusion MRI data have been used in the past as indications of WM integrity [1], [5]. Though these have proven successful in many applications, they give ambiguous or misleading results in some relatively common cases [6], and they all measure tightly localized tissue properties. It is conceivable that widely distributed damage could significantly affect the overall function of the WM even while insignificantly affecting such a local measure at each point. Since psychiatric pathologies may arise from disrupted WM functioning, rather than directly from local tissue damage, we seek a more "holistic" quantitative measure of the WM.

II. Methods

Given two volumes of interest (VOIs) in the a nonuniform anisotropic diffusive medium—the brain, for example—we define connective coherence (CC) as the log of the ratio of the observed diffusion to the diffusion expected in the null case of a standard uniform isotropic medium. We measure diffusion as the percentage of a virtual tracing compound emitted from one VOI that reaches the other.

If $CC = 0$, then the observed diffusion in the medium and the null case are equivalent, indicating that no organized (*i.e.* nonrandom) internal structure that affects diffusion between the VOIs is present in the medium. $CC > 0$ indicates that the internal structure promotes diffusion between the VOIs, while $CC < 0$ indicates that the internal structure inhibits diffusion between. Note that CC does not specify the location or orientation of the structure, but rather the aggregate effect it has upon diffusion between the VOIs.

We are currently developing visualization software for brain diffusion datasets that allows the interactive selection of cortical regions by "painting" in two dimensions upon the exposed surface of the brain. After the user selects two cortical regions, the software generates VOIs and computes CC between them by Monte Carlo diffusion simulation in the nonuniform case and by solving the heat equation in the uniform case.

III. Validation

We hypothesize that connective coherence is a meaningful measure for indicating white matter integrity, and we have designed an experiment to test this hypothesis. We first define three cortical regions of interest: Broca's area, Wernicke's area, and the superior primary motor cortex. The first two regions are involved in speech processing and are connected by the arcuate fasciculus WM tract, while the third controls the movement of the legs and feet. A domain expert uses the visualization software to select equal-area regions of interest corresponding to these three on each brain in a population of CADASIL patients and a matched population of normal controls. For each patient, we then compute CC_1 between Broca's and Wernicke's areas and CC_2 between Broca's area and the motor cortex. If CC is a good measure of WM integrity, we expect CC_1 in the normal population to be significantly greater than both CC_2 in the normal population and CC_1 in the CADASIL population.

IV. Conclusion

Connective coherence is an appealing alternative to localized measures of white matter integrity for a variety of abstract reasons, but is as yet unproven as a valid and useful neuroscience tool. Pending validation, CC is expected to be useful in neuropsychiatric research, as its mathematical properties are more suited to address the functional quality of white matter connections than other measures.

References

[1] Basser,*et al. J. of Magn. Res.*, 111:209–219, 1996.
[2] Davatzikos,*et al. Cerebral Cortex*, 12(7):767–771, Jul 2002.
[3] Friston,*et al. Clin. Neuroscience*, 3(2):89–97, 1995.
[4] Grant,*et al. Neuroimaging*, 147(2–3):233–237, Oct 2006.
[5] Kim,*et al. Neuroreport*, 16(10):1049–1053, Jul 2005.
[6] Pierpaoli,*et al. Magn. Res. Med.*, 36:893–906, Dec 1996.
[7] Villarreal,*et al. Sem. Clin. Neuropsychiatry*, 6:131–145, Apr 2001.